

Substrate Specificity, Processivity, and Kinetic Mechanism of Protein Arginine Methyltransferase 5

Min Wang,[†] Rui-Ming Xu,[‡] and Paul R. Thompson^{*,†,§}

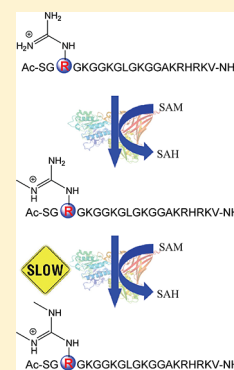
[†]Department of Chemistry, The Scripps Research Institute, 130 Scripps Way, Jupiter, Florida 33458, United States

[‡]National Laboratory of Biomacromolecules, Institute of Biophysics, Chinese Academy of Sciences, Beijing 100101, China

[§]The Kellogg School of Science and Technology, The Scripps Research Institute, Scripps Florida, Jupiter, Florida 33458, United States

S Supporting Information

ABSTRACT: Protein arginine methyltransferases (PRMTs) have emerged as attractive therapeutic targets for heart disease and cancers. PRMT5 is a particularly interesting target because it is overexpressed in blood, breast, colon, and stomach cancers and promotes cell survival in the face of DNA damaging agents. As the only known member of the PRMT enzyme family to catalyze the formation of mono- and symmetrically dimethylated arginine residues, PRMT5 is also mechanistically unique. As a part of a program to characterize the mechanisms and regulation of the PRMTs and develop chemical probes targeting these enzymes, we characterized the substrate specificity, processivity, and kinetic mechanism of bacterially expressed *Caenorhabditis elegans* PRMT5 (cPRMT5). In this report, we demonstrate that distal positively charged residues contribute to substrate binding in a synergistic fashion. Additionally, we show that cPRMT5 catalyzes symmetric dimethylation in a distributive fashion. Finally, the results of initial velocity, product, and dead-end inhibition studies indicate that cPRMT5 uses a rapid equilibrium random mechanism with dead-end EAP and EBQ complexes. In total, these studies will guide PRMT5 inhibitor development and lay the foundation for studying how the activity of this medically relevant enzyme is regulated.



Over the past decade, arginine methylation has emerged as an important post-translational modification (PTM), and several of the enzymes that catalyze this PTM (i.e., the protein arginine methyltransferase (PRMTs)) appear to be attractive therapeutic targets for a variety of human ailments including heart disease and cancer.^{1–6} There are nine human PRMTs (PRMTs 1–9),⁷ and these enzymes catalyze the monomethylation (MMA) and asymmetric (ADMA) or symmetric dimethylation of arginine (SDMA) residues. PRMTs 1, 2, 3, 4, and 6 produce both MMA and ADMA, in which two methyl groups are transferred to the same ω -nitrogen, whereas PRMT5 catalyzes the formation of MMA and SDMA, where two methyl groups are transferred to two separate ω -nitrogens (Figure 1). PRMT7 is the only known example of a PRMT that solely generates monomethyl arginine.⁸ Hundreds of PRMT substrates have been identified, and given their diversity as well as the important role that arginines play in protein–protein and protein–nucleic acid interactions, it is unsurprising that these enzymes control numerous cellular processes, including gene transcription, DNA repair, RNA splicing, and kinase signaling.^{7,9,10}

Given the essential role of the PRMTs in these processes, it should not be surprising that when dysregulated, these enzymes contribute to disease pathology. PRMT5 is a particularly attractive target for the development of an anticancer therapeutic because this enzyme, which is important for cell growth and proliferation, is overexpressed in cancers of the blood, breast, colon, and stomach.^{10–14} Although it is unclear

how PRMT5 activity contributes to tumorigenesis, several recent studies have highlighted potential mechanisms. For example, PRMT5 methylates the tumor suppressor p53 at R333, R335, and R337 in response to DNA damage, and this modification regulates the p53 response by altering its promoter specificity. One consequence is the increased expression of the cyclin-dependent kinase inhibitor p21 and decreased expression of pro-apoptotic proteins such as NOXA and PUMA.¹⁵ Consistent with this effect, siRNA knockdown of PRMT5 led to enhanced apoptosis in response to DNA damage.¹⁵ Further supporting a role for this particular PTM in cancer biology is the fact that R337, one of the sites of modification, is mutated in Li Fraumeni syndrome, a rare genetic disorder that is associated with an increased risk of developing several types of cancer.^{16,17} In a related study,¹⁴ the same authors showed that PRMT5 methylates E2F1 at R111 and R113, and methylation of these residues promotes E2F1 ubiquitination and degradation. Importantly, siRNA knockdown of PRMT5 stabilized E2F1, especially in the presence of DNA damaging reagents, and these effects were correlated with increased apoptosis. Combined with the p53 studies, these data suggest that PRMT5 promotes cell survival in response to DNA damaging agents by upregulating the p53 dependent expression of cell cycle inhibitors (e.g., p21), and by promoting the

Received: April 24, 2013

Revised: June 20, 2013

Published: July 18, 2013

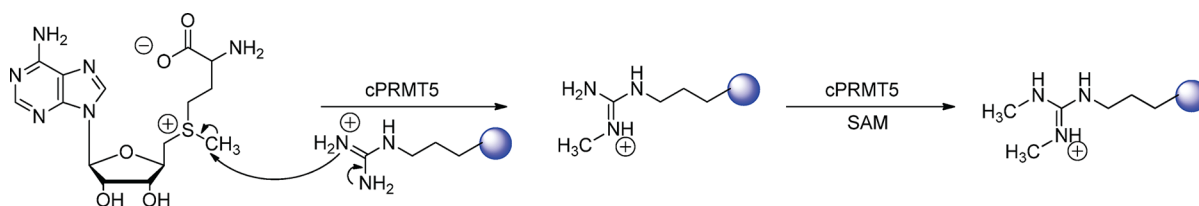


Figure 1. cPRMT5 catalyzed methylation reaction.

degradation of E2F1, thereby preventing the increased transcription of proapoptotic effectors. In total, these data suggest that PRMT5 inhibitors are likely to promote cell cycle arrest and apoptosis alone or in combination with a DNA damaging agent.

Additional evidence supporting a role for PRMT5 in oncogenesis is the observation that high levels of PRMT5 and low E2F1 levels correlate with worse outcomes in colorectal cancer.¹⁴ Similarly, high expression of both PRMT5 and the tumor suppressor protein programmed cell death 4 (PDCD4) is associated with the decreased survival of breast cancer patients.¹⁸ In fact, coexpression of these two proteins synergistically enhances the growth of MCF7e tumor xenografts. The PRMT5 catalyzed methylation of PDCD4 (at R110) is required for this effect because a PRMT5 mutant or a non-methylatable PDCD4 mutant do not promote xenograft growth.¹⁸ Aggarwal et al. reported another case in which PRMT5 acts as an oncoprotein.¹⁹ Specifically, the authors showed that cyclin D1/CDK4 kinase phosphorylates Thr5 on methylome protein 50 (MEP50), a PRMT5 interacting protein, and increases the methyltransferase activity of the PRMT5-MEP50 complex. The increased activity results in the decreased expression of CUL4A/B, the E3 ubiquitin ligase responsible for promoting the degradation of the replication licensing protein CDT1. As a consequence, CDT1 accumulates and promotes DNA rereplication, triggering the DNA damage-checkpoint and promoting malignant transformation.¹⁹ Moreover, PRMT5 is recruited to the promoters of several other tumor suppressor genes, for example, ST7 and NM23, where it methylates histone H3 (at R8) and H4 (at R3) to promote a chromatin state that is refractory to transcription.²⁰

Given the extensive links between PRMT5 and tumorigenesis, we and others have initiated programs to understand the mechanisms of catalysis and develop inhibitors targeting PRMT5. Previous work on this enzyme includes the determination of the structure of the *Caenorhabditis elegans* orthologue (cPRMT5), which shares 34% sequence identity (and 48% similarity) with human PRMT5.^{21,22} Like other PRMTs, cPRMT5 consists of a class I methyltransferase domain linked in series to a β -barrel domain that is likely important for substrate binding. In addition, the cPRMT5 structure revealed that the large N-terminal domain (residues 42–439) is structurally homologous to a TIM barrel. While it is not known whether the TIM barrel has any intrinsic activity, it is important for the PRMT5-MEP50 interaction, as revealed by the structure of the PRMT5-MEP50 complex.^{23,24} In contrast to the cPRMT5, the human orthologue displays low activity toward histones H3 and H4 unless complexed with MEP50; cPRMT5 shows high histone H4 activity in the absence of an interacting protein *vide infra*. In addition to MEP50, PRMT5 interacts with numerous other binding proteins alone and in combination with MEP50 that likely regulate PRMT5 activity either directly or by targeting the enzyme to specific substrates.

For example, CORP5 (cooperator of PRMT5) binds PRMT5 and biases its activity toward histone H3.²⁵

Although PRMT5 is structurally well characterized, limited kinetic and mechanistic studies have been performed on this enzyme. For example, it is unclear how PRMT5 symmetrically dimethylates its substrates as is the molecular basis for how interacting proteins and PTMs regulate its activity. Toward a deeper understanding of these features of PRMT5 catalysis, we initiated studies on the *C. elegans* orthologue. Our initial efforts focused on this enzyme because it shares strong sequence identity (34%) to the human enzyme, and knockdown of PRMT5 in *C. elegans* increases its sensitivity to DNA damaging agents by altering the promoter specificity of CEP-1, the p53 worm orthologue, similar to what occurs with the human enzyme.²² Additionally, cPRMT5 can be expressed in decent yield in bacteria,²¹ whereas hPRMT5 must be coexpressed with MEP50 in insect or human cells.²³ Herein we report the results of our initial efforts, including our demonstration that, like PRMT1 and PRMT6,²⁶ long-range interactions are important for PRMT5 substrate recognition. We also show that dimethylation occurs in a distributive fashion and that formation of the dimethylated peptide does not occur until the concentration of the monomethylated product exceeds that of the unmodified substrate; this effect is likely due to the high K_M for the monomethylated peptide. Finally, we demonstrate that PRMT5 uses a rapid equilibrium random kinetic mechanism with dead-end EAP and EBQ complexes. In total, these studies lay the foundation for future drug discovery efforts, as well as efforts to understand how this enzyme is regulated.

■ EXPERIMENTAL PROCEDURES

Reagents. *N*-(2-Hydroxyethyl)piperazine-*N'*-(2-ethanesulfonic acid) (HEPES), tricine, and dithiothreitol (DTT) were purchased from Research Products International Corp. Tris-(hydroxyl-methyl)aminomethane (tris) was purchased from Bio-Rad. Ethylenediamine tetraacetic acid (EDTA) and trifluoroacetic acid (TFA) were from EMD. *N*- α -Fmoc amino acids and preloaded Wang-based resins were purchased from Novabiochem. ¹⁴C-Labeled bovine serum albumin (BSA) and piperidine were purchased from Sigma-Aldrich. ¹⁴C-Methyl-SAM (56.3 mCi/mmol; 355 μ M) was purchased from Perkin-Elmer Life Sciences. Histone H4 was purified as described.²⁷ The synthesis of the AcH4-21R3MMA, AcH4-21R3ADMA, AcH4-14, AcH4-18, RGG3, AcH4-21S1A, AcH4-21K16A, AcH4-21R17A, AcH4-21R17K, AcH4-21H18A, AcH4-21H18K, AcH4-21H18Q, AcH4-21R19A, AcH4-21R19K, AcH4-21K20A, AcH4-21R17,19A and AcH4-21R17,19K peptides was previously described.²⁸

Purification of cPRMT5. cPRMT5 was expressed in *Escherichia coli* BL21(DE3) cells, using a previously described pET21a expression vector (Novagen)²¹ that encodes full-length cPRMT5 linked to a C-terminal poly(His)-tag. For protein

expression, starter cultures plus 100 $\mu\text{g/mL}$ ampicillin were grown overnight, and the following day these cultures were used to inoculate 3×2 L LB media containing 100 $\mu\text{g/mL}$ of ampicillin. The cells were then grown at 37°C for 4 h at 200 rpm to an OD_{600} of 0.6. Protein expression was then induced by the addition of IPTG (0.2 mM final). After incubation for 24 h at 16°C and 170 rpm, the cells were harvested by centrifugation (7440g for 15 min at 4°C). The cell paste was resuspended in 60 mL of lysis buffer (20 mM HEPES at pH 8.0, 50 mM NaCl, 0.5 mM phenylmethylsulfonyl fluoride, 1% Triton X-100, 1 mg/mL lysozyme, and 1 unit/mL benzonase) and incubated with rocking for 30 min. The resulting cell lysate was centrifuged at 30720g for 30 min at 4°C , and the supernatant containing cPRMT5 was applied to a nickel(II) chelating Sepharose column. The column was washed with a stepwise elution buffer containing 0 to 1 M imidazole in 20 mM HEPES at pH 8.0 plus 50 mM NaCl. Fractions were analyzed by SDS-PAGE, and fractions containing protein were combined and loaded on to a Mono Q anion exchange column (GE Healthcare) and then purified by FPLC. The target protein was eluted with 20 mM HEPES, pH 8.0, using a 0.1–0.25 M linear gradient of NaCl. The protein containing fractions were concentrated with a 10 kDa Amicon Centrifuplus centrifugal filter device. Imidazole was removed by dialysis in 50 mM HEPES at pH 8.0 plus 100 mM NaCl, 1 mM DTT, 2 mM EDTA, and 10% glycerol. Protein purity (>95%) was verified by SDS-PAGE (Figure S1, Supporting Information), and the concentration was determined using the Bradford method. The yield was 0.1 mg per 1 g of wet cells.

Synthesis of Histone-Based Peptide Substrates and Inhibitors. Peptides were synthesized on a Rainin PS3 automated peptide synthesizer using commercially available amino acids and Wang-based resins. The peptides were then cleaved from the resin with 10 mL of 95% TFA, 2.5% TIS, and 2.5% water. The peptides were then precipitated with diethyl ether, resuspended in 25 mL of ddH_2O , frozen, and then lyophilized overnight before purification by reverse phase HPLC. MALDI MS was used to verify the structure of the peptides (AcH4-21 calculated m/z is 2132, observed m/z is 2133; AcH4-21R3SDMA calculated m/z is 2160, observed m/z is 2161; AcH4-21R3K, calculated m/z is 2104, observed m/z is 2105). Peptide concentrations were determined by titrating peptides with methyltransferase assays using PRMT1 or cPRMT5 as the catalyst. Briefly, limiting amounts of an individual peptide were reacted with a ≥ 6 -fold excess of ^{14}C -SAM (based on mass), and the reaction was monitored as a function of time until completion. The amount of product formed was used to correct the substrate concentration, assuming one or two methylation events for substrates modified by cPRMT5 and PRMT1, respectively.

Mass Spectrometry Based Methylation Assay. The time course for the cPRMT5 catalyzed methylation of the AcH4-21 peptide was monitored by MALDI-MS.²⁸ Briefly, the peptide substrate (20 μM) and SAM (100 μM) were preincubated at 25°C for 10 min in 50 mM HEPES, pH 8.0, 50 mM NaCl, 1 mM EDTA, and 0.5 mM DTT. We used 25°C as our assay temperature because we observed a rapid loss in activity at 37°C . The reaction was initiated by the addition of 1 μM cPRMT5 and quenched at various times with 3 μL of 50% TFA in ddH_2O at the appropriate time. The enzyme was removed, and the samples were desalted with a C-18 Zip Tip. The samples were then mixed with a saturated solution of α -cyano-4-hydroxy cinnamic acid in 50% acetonitrile, 50% water,

and 0.1% TFA and spotted onto a MALDI plate and analyzed in the positive ion mode. The percentage turnover was calculated as previously described.²⁸

Gel-Based Activity Assay. The methyltransferase activity of cPRMT5 was determined with a discontinuous gel-based assay, using methods similar to those described for PRMT1.²⁸ Briefly, Assay Buffer (50 mM HEPES at pH 8.0, 50 mM NaCl, 1 mM EDTA, and 0.5 mM dithiothreitol), containing a peptide substrate and ^{14}C -labeled SAM, was incubated for 10 min at 25°C . The reaction was then initiated by the addition of cPRMT5 (200 nM final) and quenched with $6\times$ tris–tricine gel loading dye after 10 min. Samples were loaded on to 16.5% tris–tricine polyacrylamide gels to separate methylated protein/peptide from unreacted SAM. The gels were then dried, and the incorporated radioactivity was quantified by phosphorimage analysis using a Typhoon scanner. The assays were carried out in duplicate, the standard deviations of individual replicates were generally less than 20%, and only values with less than 20% error were used in fits of the data to the equations outlined below. Initial rates were fit to eq 1,

$$v = V_{\max}[S]/([S] + K_M) \quad (1)$$

where v is the initial rate, V_{\max} is the maximum velocity, $[S]$ is the substrate concentration, and K_M is the Michaelis constant. The k_{cat} was calculated from the ratio of V_{\max} and enzyme concentration.

Initial Velocity Studies. Using the assay described above, the initial rates for ^{14}C -SAM were examined at different fixed concentrations of the AcH4-21 peptide (10, 20, 50, and 100 μM). For reactions in which the AcH4-21 peptide was the varied substrate, the initial rates were obtained at fixed concentrations of ^{14}C -SAM (5, 10, 15, and 30 μM). The initial rate data were then globally fit to eq 3,

$$v = V_{\max}[A][B]/(K_{\text{ia}}K_{\text{b}} + K_{\text{b}}[A] + K_{\text{a}}[B] + [A][B]) \quad (3)$$

where V_{\max} is the maximum velocity at saturating concentrations of the AcH4-21 peptide and SAM. K_{ia} is the dissociation constant of the varied substrate. K_{a} and K_{b} are the Michaelis constants for the varied and fixed substrates, respectively.

Inhibition Studies. The AcH4-21R3SDMA peptide and SAH were used as the product inhibitors. The dead-end analogues are sinefungin and the AcH4-21R3K peptide, a mutant peptide in which Arg3, the site methylated by PRMT5, is replaced with a lysine. The initial rate data obtained from these inhibition experiments were globally fit to eqs 4, 5, 6, and 7 for competitive, noncompetitive, mixed, and uncompetitive inhibition, respectively.

$$v = V_{\max}[S]/([S] + K_M(1 + [I]/K_{\text{is}})) \quad (4)$$

$$v = V_{\max}[S]/([S](1 + [I]/K_{\text{i}}) + K_M(1 + [I]/K_{\text{i}})) \quad (5)$$

$$v = V_{\max}[S]/([S](1 + [I]/K_{\text{ii}}) + K_M(1 + [I]/K_{\text{is}})) \quad (6)$$

$$v = V_{\max}[S]/([S](1 + [I]/K_{\text{ii}}) + K_M) \quad (7)$$

V_{\max} is the maximum velocity of the uninhibited reaction, and K_{ii} and K_{is} are the inhibition constants for the intercept and slope, respectively. Noncompetitive inhibition data were fit to eq 5, where $K_{\text{i}} = K_{\text{ii}} = K_{\text{is}}$.

Table 1. Substrate Specificity

substrate	sequence	K_M (μM)	k_{cat} (min^{-1})	k_{cat}/K_M ($\text{M}^{-1} \text{min}^{-1}$)
histone H4 ^a		22 ± 3	0.21 ± 0.01	9500 ± 1300
histone H3 ^{a,c}				<50 ± 6
AcH4-21 ^a	Ac-SGRGKGGKGLGKGGAKRHRKV	13 ± 2	1.2 ± 0.01	92000 ± 14000
SAM ^b		5.3 ± 0.2	1.1 ± 0.01	210000 ± 8000
RGG3 ^a	GGRGGFGGRGGFGRGGFG	130 ± 8	0.21 ± 0.01	1600 ± 100
AcH4-21R3K ^{a,c}	Ac-SGKGKGGKGLGKGGAKRHRKV			<24.5 ± 3
AcH4-21R3MMA ^a	Ac-SGR ^(Me) GKGGKGLGKGGAKRHRKV	390 ± 50	0.22 ± 0.01	570 ± 70
AcH4-21R3SDMA ^{a,c}	Ac-SGR ^{(Me)2} GKGGKGLGKGGAKRHRKV			<15.2 ± 2
AcH4-21R3ADMA ^{a,c}	Ac-SGR ^{(Me)2} GKGGKGLGKGGAKRHRKV			<17.9 ± 3

^a[SAM] = 15 μM . ^b[AcH4-21] = 100 μM . ^cThe amount of product formation was too low to accurately measure the kinetic parameters for this peptide substrate. Therefore an estimation of k_{cat}/K_M was made by dividing the maximal observed rate by the concentration of substrate.

Table 2. Mutagenesis Studies

substrate ^a	sequence	K_M (μM)	k_{cat} (min^{-1})	k_{cat}/K_M ($\text{M}^{-1} \text{min}^{-1}$)
AcH4-21	Ac-SGRGKGGKGLGKGGAKRHRKV	13 ± 2	1.2 ± 0.01	$9.2 \times 10^4 \pm 1.3 \times 10^3$
AcH4-18	Ac-SGRGKGGKGLGKGGAKRH	310 ± 40	0.27 ± 0.01	$8.7 \times 10^2 \pm 1.1 \times 10^2$
AcH4-14	Ac-SGRGKGGKGLGKGG			<22.3 ± 6
AcH4-21S1A	Ac-AGRGKGGKGLGKGGAKRHRKV	15 ± 2	0.95 ± 0.02	$6.3 \times 10^4 \pm 8.0 \times 10^3$
AcH4-21K16A	Ac-SGRGKGGKGLGKGGAAHRKV	21 ± 3	0.46 ± 0.01	$2.1 \times 10^4 \pm 3.0 \times 10^3$
AcH4-21R17A	Ac-SGRGKGGKGLGKGGAKAHRKV	84 ± 6	0.95 ± 0.02	$1.1 \times 10^4 \pm 8.0 \times 10^2$
AcH4-21R17K	Ac-SGRGKGGKGLGKGGAKKHRKV	230 ± 30	0.89 ± 0.04	$3.9 \times 10^3 \pm 5.0 \times 10^2$
AcH4-21H18A	Ac-SGRGKGGKGLGKGGAKRARKV	54 ± 8	0.53 ± 0.02	$9.8 \times 10^3 \pm 1.5 \times 10^3$
AcH4-21H18K	Ac-SGRGKGGKGLGKGGAKRKRKV	190 ± 15	0.75 ± 0.02	$4.0 \times 10^3 \pm 3.0 \times 10^2$
AcH4-21H18Q	Ac-SGRGKGGKGLGKGGAKRQRKV	610 ± 113	1.0 ± 0.09	$1.6 \times 10^3 \pm 3.0 \times 10^2$
AcH4-21R19A	Ac-SGRGKGGKGLGKGGAKRHAKV	120 ± 16	0.29 ± 0.01	$2.4 \times 10^3 \pm 3.0 \times 10^2$
AcH4-21R19K	Ac-SGRGKGGKGLGKGGAKRHKKV	43 ± 8	0.53 ± 0.03	$1.2 \times 10^4 \pm 2.0 \times 10^3$
AcH4-21K20A	Ac-SGRGKGGKGLGKGGAKRHRAV	31 ± 4	0.52 ± 0.02	$1.7 \times 10^4 \pm 2.0 \times 10^3$
AcH4-1R17,19A	Ac-SGRGKGGKGLGKGGAKAHAKV	95 ± 10	0.94 ± 0.03	$9.9 \times 10^3 \pm 1.0 \times 10^3$
AcH4-1R17,19K	Ac-SGRGKGGKGLGKGGAKKHKKV	195 ± 19	0.70 ± 0.02	$3.6 \times 10^3 \pm 3.0 \times 10^2$

^a[SAM] = 15 μM .

RESULTS

cPRMT5 Methylation of Protein Substrates. Using a discontinuous gel-based radioactive assay, we determined the steady-state kinetic parameters for both histone H3 and histone H4, which are known PRMT5 substrates.^{20,29} While cPRMT5 shows decent activity toward histone H4 ($k_{\text{cat}}/K_M = 9.5 \times 10^3 \text{ M}^{-1} \text{min}^{-1}$), histone H3 is an extremely poor cPRMT5 substrate ($k_{\text{cat}}/K_M \leq 50 \text{ M}^{-1} \text{min}^{-1}$). With respect to histone H4, the observed k_{cat}/K_M value is comparable to those previously established for the *C. elegans* enzyme ($9.5 \times 10^3 \text{ M}^{-1} \text{min}^{-1}$ versus $2.4 \times 10^4 \text{ M}^{-1} \text{min}^{-1}$).²¹ Relative to PRMT1, however, the k_{cat}/K_M is 20-fold lower.²⁸ The decreased activity is primarily a K_M effect as the k_{cat} is only decreased by 2-fold relative to PRMT1; the small change in k_{cat} is likely due to the decreased assay temperature (25 °C for cPRMT5 versus 37 °C for PRMT1). In contrast, the K_M for histone H4 is 10-fold higher than that obtained with PRMT1, indicating that histone H4 is a relatively poorer substrate for cPRMT5 than for PRMT1.

cPRMT5 Methylation of Peptide-Based Substrates. Given that PRMT5 methylates histone H4 at R3 in the unstructured N-terminal tail region of the protein, we also determined the steady-state kinetic parameters for the AcH4-21 peptide, whose sequence mimics the N-terminus of histone H4. The results of these experiments indicate that the AcH4-21 peptide is an excellent PRMT5 substrate, with a k_{cat}/K_M that is ~10 fold higher ($9.2 \times 10^4 \text{ M}^{-1} \text{min}^{-1}$) than that obtained for the parent protein histone H4. In contrast, the RGG3 peptide,

whose sequence is based on fibrillarlin and which has classically been used to study PRMT activity, is a significantly poorer substrate ($k_{\text{cat}}/K_M = 1.6 \times 10^3 \text{ M}^{-1} \text{min}^{-1}$). The steady-state kinetics were also determined for SAM, and these values are comparable to those obtained for other PRMTs including PRMTs 1 and 6.^{26,28} The fact that cPRMT5 modifies the AcH4-21 peptide comparably to or even better than histone H4 indicated that this peptide, which contains the major *in vivo* site of PRMT5 catalyzed methylation, that is R3,²⁵ could be used to study the regiospecificity of the enzyme and identify specific residues that are important for substrate recognition.

Regiospecificity of cPRMT5. In order to confirm that cPRMT5 methylates arginine 3 in the context of the AcH4-21 peptide, we determined whether the AcH4-21R3K peptide was a substrate for cPRMT5; R3 is mutated to a lysine in this peptide (Table 1). The fact that AcH4-21R3K peptide is essentially not processed by the enzyme ($k_{\text{cat}}/K_M < 24.5 \text{ M}^{-1} \text{min}^{-1}$) verified that cPRMT5 preferentially modifies R3 in the AcH4-21 peptide and not the two other arginines in this peptide, that is, R17 and R19. To validate this finding, we determined the kinetic parameters for the AcH4-21R3SDMA and AcH4-21R3ADMA peptides, which contain symmetrically and asymmetrically dimethylated arginine in place of R3, and demonstrated that they are also extremely poor substrates ($k_{\text{cat}}/K_M < 15.2$ and $17.9 \text{ M}^{-1} \text{min}^{-1}$, respectively). In contrast, the monomethylated peptide (i.e., AcH4-21R3MMA) is processed by the enzyme ($k_{\text{cat}}/K_M = 5.7 \times 10^2 \text{ M}^{-1} \text{min}^{-1}$), albeit at a much reduced rate; the k_{cat}/K_M for this peptide is decreased by

~160-fold relative to the AcH4-21 peptide. The decreased k_{cat}/K_M is largely driven by a ~35-fold increase in K_M . While this result provides further support for the symmetric dimethylation of R3, it also indicates that the efficiency of adding a second methyl group to this residue is very low. Nevertheless the fact that cPRMT5 regiospecifically modifies the AcH4-21 peptide at R3 with comparable kinetics to the parent protein further indicated that this peptide provides an excellent model system to study the substrate specificity and kinetic mechanism of the enzyme.

Substrate Recognition Elements. Having established the AcH4-21 peptide as a model system, we moved forward and tested a number of “mutant” peptides to identify specific elements that are important for substrate recognition (Table 2). Initially, we determined the kinetic parameters for two truncation mutants, that is, the AcH4-18 and AcH4-14 peptides. The results of these experiments demonstrated that both peptides are significantly (100–4000-fold) poorer substrates for the enzyme than the AcH4-21 peptide (Table 2). These results suggest that, like PRMT1,²⁸ residues distal to the site of methylation are important for substrate recognition. To support this notion, we examined the kinetic parameters of a series of C-terminal “mutant” peptides, focusing on the polar and charged residues in this region, that is, K¹⁶RHRK²⁰. The results of these studies (Table 2 and Figure 2B) indicate that no single residue is absolutely required for substrate recognition. For example, the effect of mutating K16 and K20 to alanine is relatively modest (4.4- and 5.5-fold reductions in k_{cat}/K_M ,

respectively). In contrast, mutation of R17, H18, and R19 had a more dramatic effect. For example, mutating R17 to the less bulky alanine decreased the k_{cat}/K_M by ~9-fold, while substitution of this residue with a lysine led to an approximate 20-fold decrease in k_{cat}/K_M . Similarly to the R17 mutants, the k_{cat}/K_M values determined for H18K and H18Q mutants are decreased by ~20-fold and ~50-fold, respectively. However, when H18 was replaced by a smaller residue, such as alanine, the k_{cat}/K_M was only decreased by ~10-fold. These results indicate that both the charge and position of R17 and H18 are important for substrate recognition by both R17 and H18. Mutation of R19 to alanine also led to a substantial (~40-fold) decrease in k_{cat}/K_M . In contrast, the k_{cat}/K_M for the R19K mutant is only decreased by ~8-fold, suggesting that the positive charge of this residue and to a lesser extent its position is important for substrate recognition. Since the total effect of mutating residues 16–20 is less than the effect of their deletion (60-fold versus 4000-fold for the AcH4-14 peptide), the C-terminus of the AcH4-21 likely contributes to substrate binding in synergistic fashion.

We additionally examined the effect of mutating S1 to alanine because this residue is proximal to the site of methylation. The results of these studies indicate that the β -hydroxyl is relatively unimportant for substrate recognition because the k_{cat}/K_M is decreased by only 1.5-fold. In total, these results are consistent with the structure of the hPRMT5·ME-P50·A9145C·AcH4-21 complex (A9145C is a SAM analog).²³ For example, residues S1 to K5 bind in a small pocket at the interface between the SAM binding and β -barrel domains. In this region, these residues adopt a tight β -turn that is stabilized by hydrogen bonds between the main chain carbonyl of S1 and the amide nitrogen of G4 and the side chain of Q309 in PRMT5. The lack of an observable interaction with the β -hydroxyl is consistent with the lack of a significant effect on k_{cat}/K_M . Unfortunately, however, electron density beyond K8 is not visible in the structure; as such, it is difficult to comment on interactions between PRMT5 and the C-terminus of the peptide. Nevertheless, the lack of significant contacts with the side chain of K8 is consistent with the C-terminus of a substrate being able to bind at a distal site on the enzyme.

cPRMT5 Methylates Substrates in a Distributive Fashion. PRMT5 is reported to catalyze the formation of monomethylated and symmetrically dimethylated arginine residues.³⁰ However, it is unknown how this reaction proceeds and whether it occurs in a processive or nonprocessive, that is, distributive, fashion. In the processive mechanism, peptide binding is accompanied by two sequential methylation events without the release of the peptide to solution. In contrast, in a distributive mechanism, the peptide is released prior to rebinding to facilitate a second round of methylation.

To address the issue of how cPRMT5 catalyzes SDMA formation, we used a previously described MALDI-MS-based assay²⁸ to monitor product formation as a function of time. As depicted in Figure 3, product formation was monitored over 3 h. At the initial time points (0, 10, and 30 min), only the MMA containing product is detectable. The appearance of the dimethylated species, which is only observable after 60 min, coincides with the loss of linearity in the AcH4-21 MMA progress course. At the later time points, where the levels of the AcH4-21 peptide are nearly exhausted, the levels of the dimethylated peptide further increase, and the levels of MMA plateau. At lower concentrations of the peptide substrate, the level of the dimethylated species rises more quickly (Figure S2,

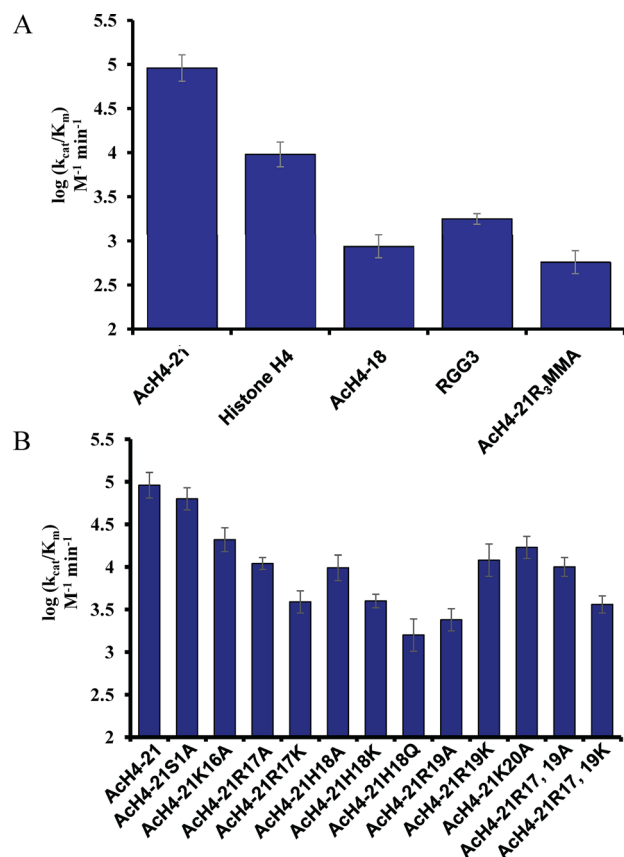


Figure 2. Substrate specificity of cPRMT5. The k_{cat}/K_M values determined for (A) histone H4 and H4 based peptides of varying length, as well as the fibrillar peptide RGG3. (B) Kinetic analysis of “mutant” AcH4-21 peptides.

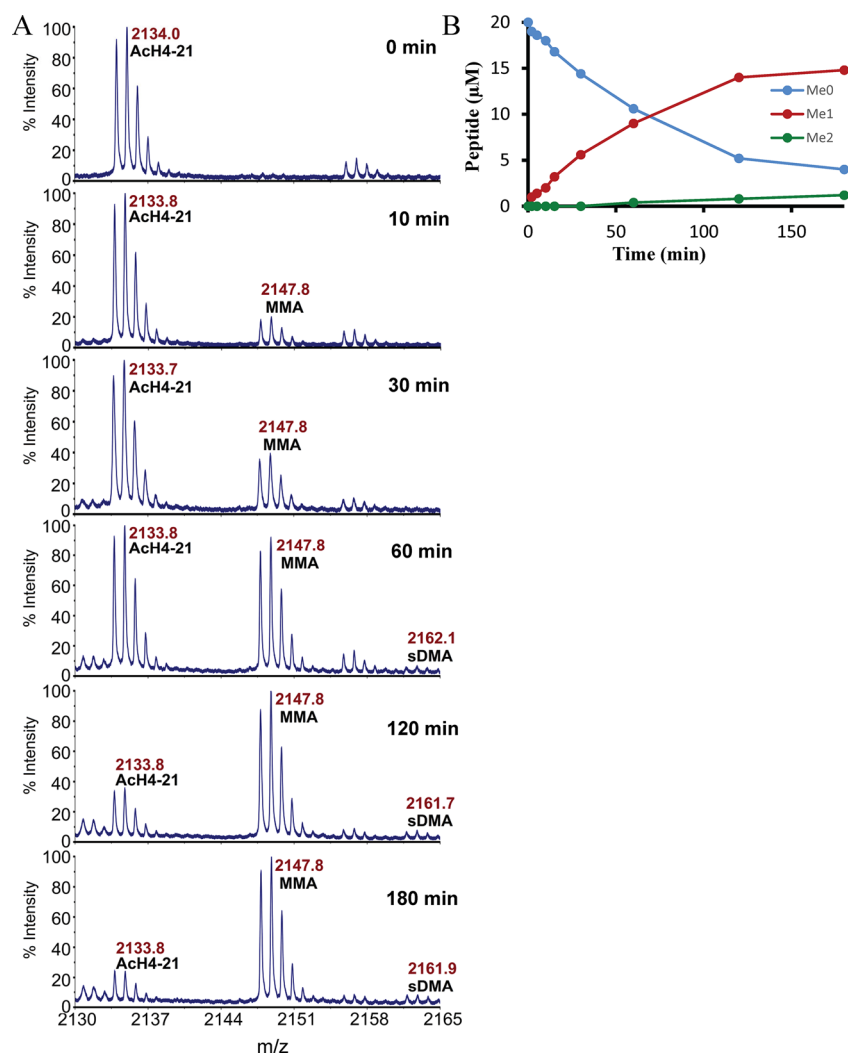


Figure 3. cPRMT5 methylates the Ach4-21 peptide in a distributive fashion. (A) Methylation of the Ach4-21 peptide monitored by MALDI-MS. (B) Time course of Ach4-21 methylation. The reaction mixture, containing 50 mM HEPES, pH 8.0, 2 mM EDTA, 200 mM NaCl, 1 mM DTT, 0.1 mM SAM, 20 μ M of Ach4-21, and 1 μ M of cPRMT5, was incubated at 25 $^{\circ}$ C over 3 h. Unmethylated (Me0), monomethylated (Me1), and dimethylated (Me2) Ach4-21 were quantified by mass spectrometry.

Table 3. Initial Velocity Studies

varied substrate	fixed substrate	k_{cat} (min^{-1})	$K_{\text{d}(\text{pep})}$ (μM)	$K_{\text{M}(\text{pep})}$ (μM)	$K_{\text{d}(\text{SAM})}$ (μM)	$K_{\text{M}(\text{SAM})}$ (μM)
AcH4-21	SAM ^a	1.4 ± 0.07	33.5 ± 8.7	7.0 ± 3.2		7.9 ± 1.0
SAM	AcH4-21 ^b	1.1 ± 0.06		7.4 ± 1.5	24.6 ± 8.7	12.7 ± 3.0

^aFixed substrate concentration = 5, 10, 15, or 30 μM . ^bFixed substrate concentration = 10, 20, 40, or 60 μM .

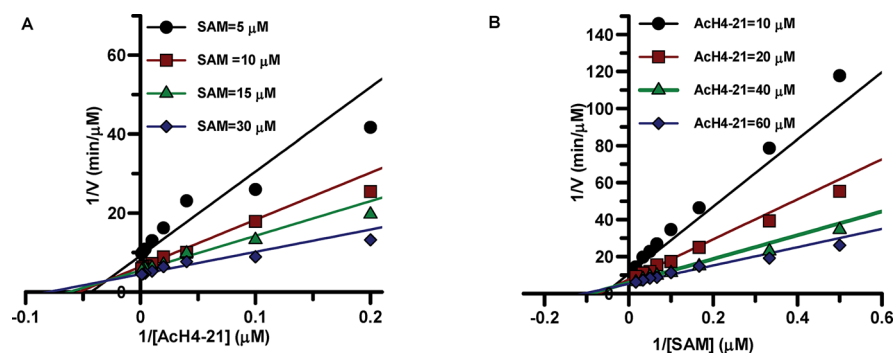


Figure 4. Initial velocity patterns. Lineweaver–Burk plots display an intersecting line pattern, indicative of a sequential mechanism, when fixed concentrations of SAM and Ach4-21 are assayed at various concentrations of the substrate, Ach4-21 (A) or SAM (B).

Supporting Information). The results suggest that cPRMT5 follows a distributive mechanism, where the monomethylated peptide is released from the enzyme and only rebinds to facilitate the second round of methylation after its levels are sufficient to compete with the unmodified peptide for binding to cPRMT5. Consistent with this conclusion is the fact that the AcH4-21R3DMA peptide is a significantly (160-fold) poorer substrate for cPRMT5, which explains the slow accumulation of the dimethylated species.

Initial Velocity Studies. To characterize the kinetic mechanism of cPRMT5, initial velocity studies were carried out. First, the concentration of the AcH4-21 peptide was varied at different fixed concentrations of the methyl donor SAM, and the initial velocities were fit to eq 3 to obtain values for $K_{M(\text{AcH4-21})}$, $K_{M(\text{SAM})}$, and $K_{d(\text{AcH4-21})}$. Similar experiments were performed with SAM as the varied substrate at different fixed concentrations of the AcH4-21 peptide to obtain values for $K_{M(\text{AcH4-21})}$, $K_{M(\text{SAM})}$, and $K_{d(\text{SAM})}$. Double reciprocal plots of the data (i.e., $1/v$ versus $1/[S]$) indicate that the lines intersect in the second quadrant (Table 3 and Figure 4). These patterns suggest that cPRMT5 uses a sequential mechanism, in which both SAM and the peptide substrate bind to cPRMT5 to form a ternary complex prior to methyl transfer.

Production Inhibition Studies. In order to determine the order of substrate binding and product release for the cPRMT5 catalyzed reaction, product inhibition studies were initiated. S-Adenosyl-homocysteine (SAH) and the AcH4-21R3DMA peptide were used as product inhibitors. The results show that SAH acts as a competitive inhibitor when the concentration of SAM is varied and the concentration of the AcH4-21 peptide is fixed at saturating levels ($50K_M$) (Table 4 and Figure 5A). The AcH4-21R3DMA peptide also acts as a competitive inhibitor when the AcH4-21 peptide was varied (Table 4 and Figure 5B), indicating that both SAM and the AcH4-21 peptide compete with SAH and the AcH4-21R3DMA peptide, respectively, for binding to the same form of enzyme. The fact that both

products act as competitive inhibitors rules out both the steady-state ordered and equilibrium ordered kinetic mechanisms.

To further define the kinetic mechanism of cPRMT5, we determined the pattern of inhibition afforded by the AcH4-21R3DMA peptide at both saturating and subsaturating levels of the AcH4-21 peptide (Table 4, and Figure 5C,D). In both cases, this peptide acts as a noncompetitive inhibitor of SAM. The observation of noncompetitive inhibition at saturating levels of the AcH4-21 peptide is inconsistent with the Theorell–Chance mechanism, as well as the rapid equilibrium random mechanism with a dead-end EBQ complex, because for both mechanisms no inhibition is predicted. The inhibition patterns are, however, consistent with a rapid equilibrium random kinetic mechanism (RER) with dead-end EAP and EBQ complexes, where A is SAM, B is the peptide substrate, P is the methylated peptide, and Q is SAH.

Dead-End Analogue Studies. To provide further evidence for the proposed kinetic mechanism, dead-end analogue studies were performed. Sinefungin, which is a SAM analogue, and the AcH4-21R3K peptide were used as the inhibitors in these studies. Sinefungin contains an amine in the place of the methyl group, whereas in the AcH4-21R3K peptide, arginine 3 is replaced with a lysine residue. As noted above the AcH4-21R3K peptide is not modified by cPRMT5.

The inhibition patterns indicate that the AcH4-21R3K peptide acts as a competitive inhibitor when the AcH4-21 peptide is varied at fixed concentrations of SAM (Table 4 and Figure 6A). When SAM is the varied substrate, the AcH4-21R3K peptide acts as a noncompetitive inhibitor at both saturating and subsaturating levels of the AcH4-21 peptide. The K_i value is, however, increased by ~20-fold at the higher concentration of the AcH4-21 peptide. Although no inhibition is predicted for the RER kinetic mechanism, the fact that the K_i value increases to $5800 \mu\text{M}$ indicates that under saturating conditions, the AcH4-21 peptide effectively out competes the AcH4-21R3K peptide for binding to the enzyme (Table 4 and Figure 6, panel B versus panel C), as is predicted for this mechanism. The results obtained when sinefungin was tested as the dead-end analog were particularly illuminating because sinefungin acts as a competitive inhibitor of SAM and a noncompetitive inhibitor of the AcH4-21 peptide (Table 4 and Figure 6D,E). The fact that neither sinefungin nor the AcH4-21R3K peptides act as uncompetitive inhibitors further rules out the Theorell–Chance mechanism and provides confirmation that cPRMT5 employs a RER kinetic mechanism with dead-end EAP and EBQ complexes (Scheme 1).

DISCUSSION

Targeted therapeutics are increasingly being used alone or in combination with other target specific inhibitors or more commonly with conventional nonselective inhibitors of cellular growth to achieve positive outcomes for a number of diseases, particularly cancer. As described above, of the various protein methyltransferases, PRMT5 has emerged as one of the most promising therapeutic targets in this class. As such, we predict that PRMT5 inhibitors, used alone or in combination with DNA damaging agents, will emerge as a key therapeutic approach for the treatment of multiple cancers. Given these links, we initiated a program to biochemically characterize the substrate specificity, processivity, and kinetic mechanism of this enzyme, with the ultimate goal being to use this information to guide inhibitor development.

Table 4. Product and Dead-End Inhibition Results for cPRMT5

inhibitor	varied substrate	fixed substrate	inhibition pattern	K_i (μM)
AcH4-21R3DMA	AcH4-21	15 μM SAM ^a	competitive	860 ± 170
AcH4-21R3DMA	SAM	1 mM AcH4-21 ^a	noncompetitive	3000 ± 220
AcH4-21R3DMA	SAM	20 μM AcH4-21 ^b	noncompetitive	310 ± 20
SAH	AcH4-21	15 μM SAM ^c	noncompetitive	5.6 ± 0.5
SAH	SAM	1 mM AcH4-21 ^c	competitive	5.1 ± 0.7
AcH4-21R3K	AcH4-21	15 μM SAM ^d	competitive	320 ± 50
AcH4-21R3K	SAM	1 mM AcH4-21 ^e	noncompetitive	5800 ± 500
AcH4-21R3K	SAM	20 μM AcH4-21 ^e	noncompetitive	300 ± 20
sinefungin	AcH4-21	15 μM SAM ^f	noncompetitive	25 ± 1.8
sinefungin	SAM	1 mM AcH4-21 ^f	competitive	9.5 ± 1.2

^a0, 1, 2, or 4 mM AcH4-21R3DMA. ^b0, 100, 250, or 500 μM AcH4-21R3DMA. ^c0, 2.5, 5, or 10 μM SAH. ^d0, 250, 500, or 1000 μM AcH4-21R3K. ^e0, 1, 2.5, or 5 mM AcH4-21R3K. ^f0, 10, 20, or 40 μM .

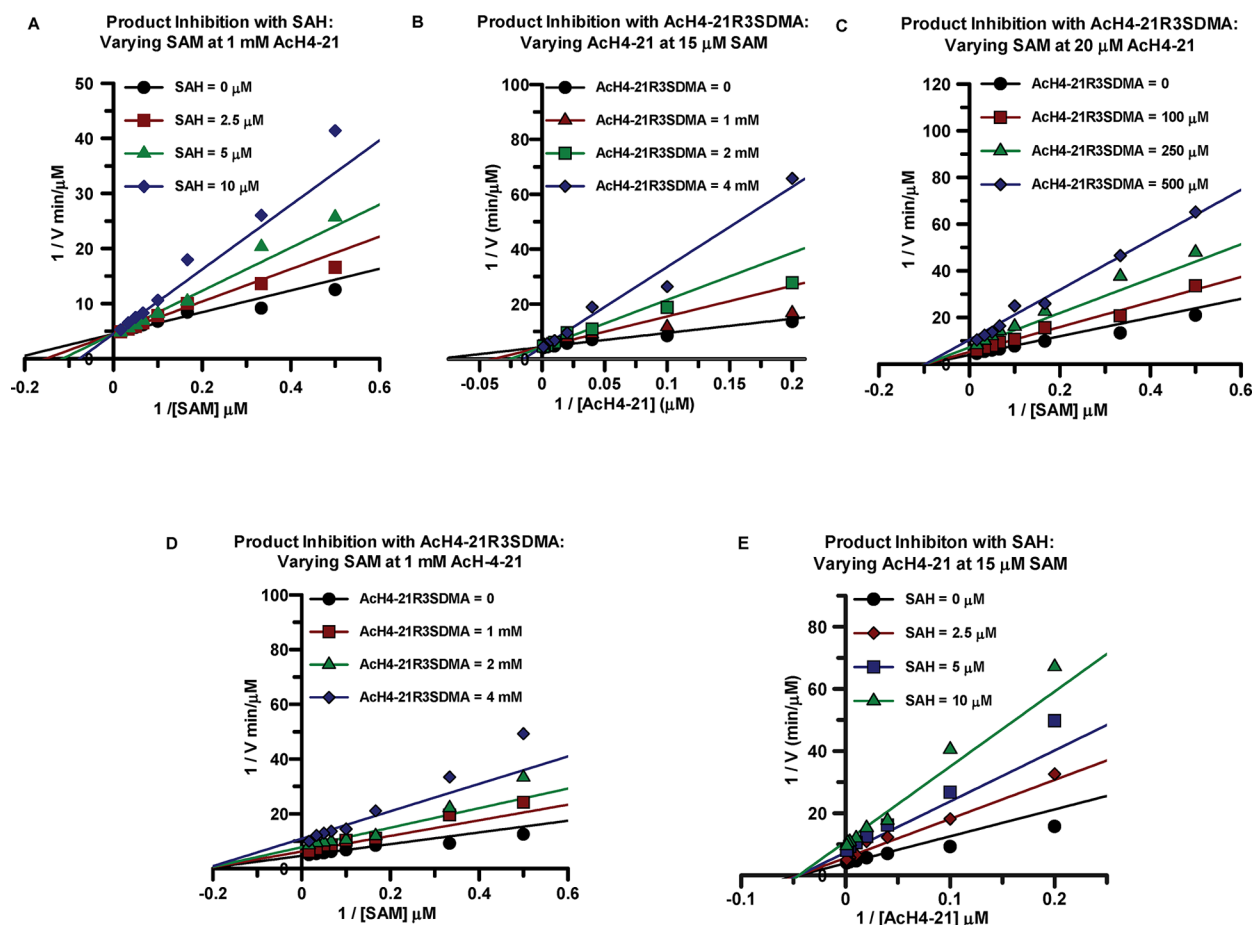


Figure 5. Product inhibition studies with SAH and AcH4-21R3SDMA. (A) Competitive inhibition is observed when SAM is the varied substrate, AcH4-21 is the fixed substrate (1 mM), and SAH is the product inhibitor. (B) Competitive inhibition is observed when AcH4-21 is the varied substrate, SAM is the fixed substrate (15 μ M), and AcH4-21R3SDMA is the product inhibitor. (C) Noncompetitive inhibition is observed when SAM is the varied substrate, AcH4-21 is the fixed substrate (20 μ M), and AcH4-21R3SDMA is the product inhibitor. (D) Weak noncompetitive inhibition is observed when SAM is the varied substrate, AcH4-21 is the fixed substrate (1 mM), and AcH4-21R3SDMA is the product inhibitor. (E) Noncompetitive inhibition is observed when AcH4-21 is the varied substrate, SAM is the fixed substrate (15 μ M), and SAH is the product inhibitor.

As a step toward that goal, we initiated studies on the *C. elegans* enzyme. We focused on this particular orthologue because cPRMT5 recapitulates many of the physiological functions of its human counterpart, including the fact that cPRMT5 knockdown increases cellular sensitivity to DNA damaging agents by altering the promoter specificity of CEP-1/p53.²² Additionally, cPRMT5 shows strong sequence homology to hPRMT5 (34% identity) but can be expressed in an autonomous fashion in bacteria. In contrast, hPRMT5 must be coexpressed with MEP50 in insect or human cells.²³ These latter points suggest that cPRMT5 can be used as a template to develop a general PRMT5 inhibitor whose potency is not affected by the various interacting proteins known to modulate PRMT5 activity and substrate specificity.

As described in detail in the Results section, and summarized here, our initial studies with cPRMT5 revealed that histone H4 is efficiently processed by the enzyme, whereas histone H3 is an extremely poor substrate, consistent with a previous study.²² Since the hPRMT5-CORP5 complex modifies histone H3, the lack of activity for this substrate likely reflects the lack of a PTM or binding partner for the *E. coli* expressed recombinant protein.

To identify a substrate that could be used for mechanistic studies, we also determined the steady-state kinetic parameters

for the AcH4-21 peptide, a histone H4 tail analog, and showed that this peptide is regiospecifically methylated at arginine 3 with comparable kinetics to the parent protein. With this substrate in hand, we further probed the substrate specificity, processivity, and kinetic mechanism of the enzyme. The results of these studies indicated that like PRMT1 and PRMT6,^{26,28} downstream positively charged residues are important for high-affinity substrate binding. Given that these three PRMTs employ similar substrate recognition mechanisms, our results imply that arginines in unstructured regions or that can adopt a β -turn are preferentially modified as long as N- or C-terminal residues provide sufficient binding energy to promote the formation of an enzyme-substrate complex that is competent for methyl transfer.

The results of our processivity studies were also quite revealing because cPRMT5 catalyzes substrate dimethylation in a distributive fashion, a conclusion that is consistent with the results obtained for hPRMT5, where MEP50 simply accelerated the rate of the reaction but did not affect the processivity.²³ In such a mechanism, the peptide is released to solution and must rebind prior to the transfer of the second methyl group. In contrast, PRMT1 catalyzes ADMA formation in a partially processive fashion;^{28,31} the reaction is termed partially processive because the forward commitment to the dimethy-

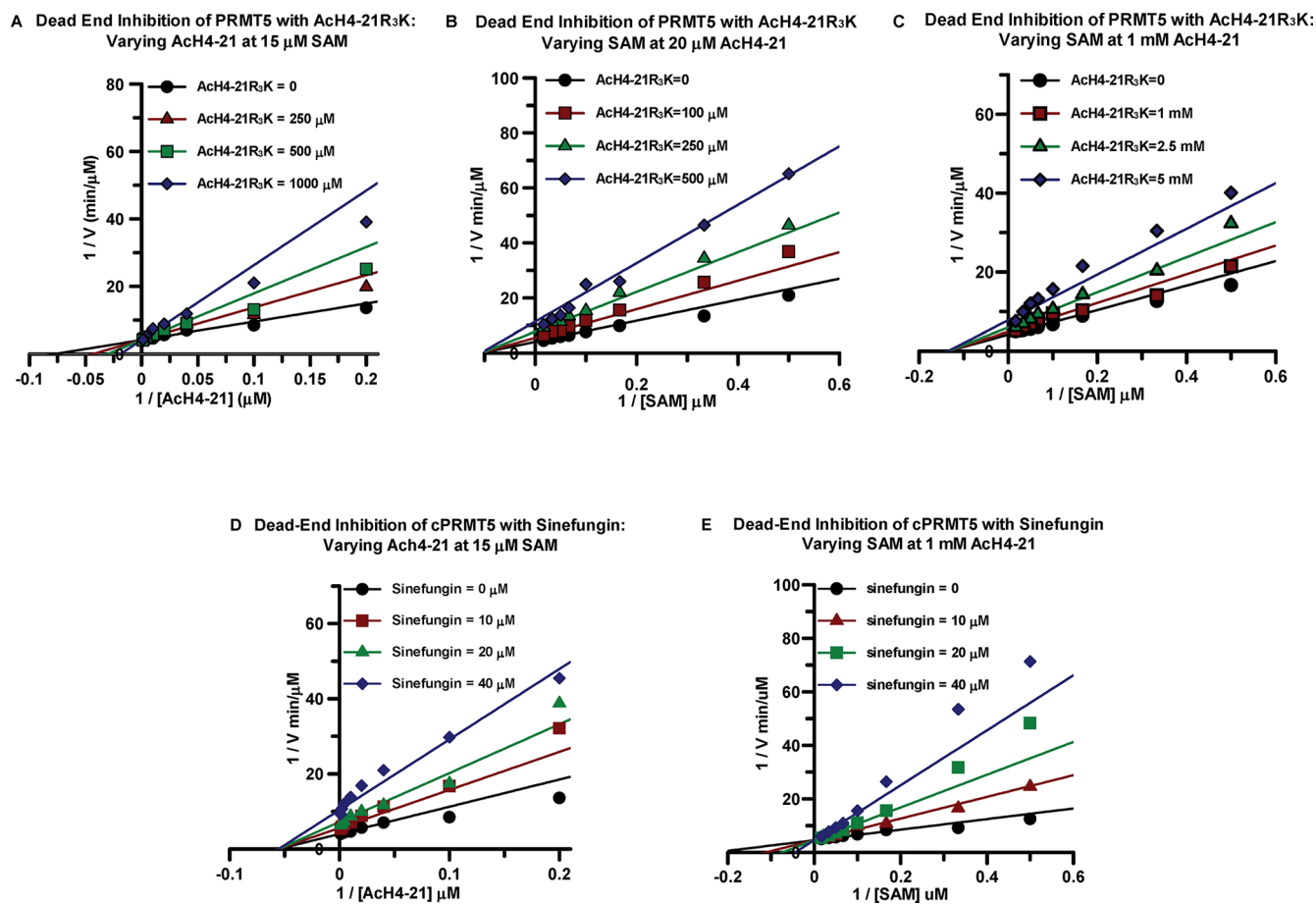
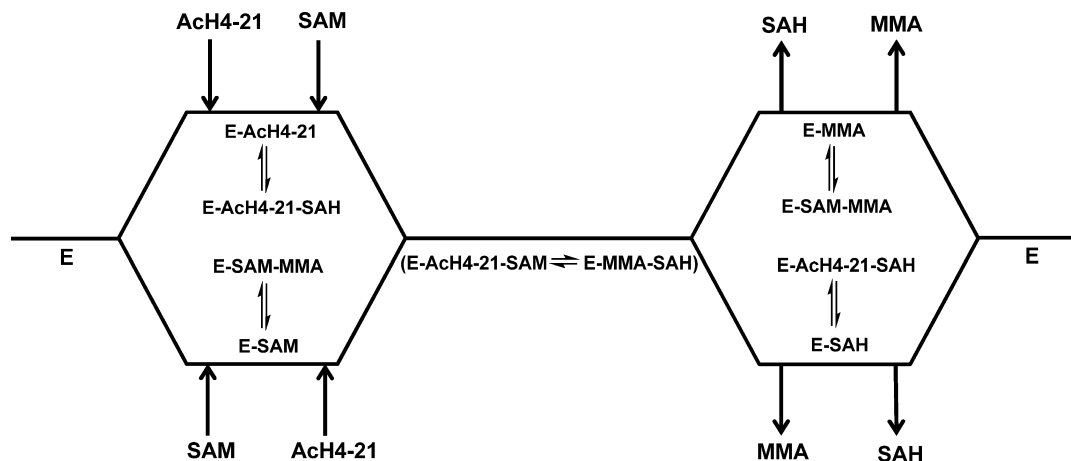


Figure 6. Dead-end analogue inhibition studies with AcH4-21R3K and sinefungin. (A) Competitive inhibition is observed when AcH4-21 is varied substrate, SAM is the fixed substrate (15 μM), and the AcH4-21R3K is the dead-end analogue inhibitor. (B) Noncompetitive inhibition is observed when SAM is the varied substrate, AcH4-21 is the fixed substrate (20 μM), and AcH4-21R3K is the dead-end analogue inhibitor. (C) Noncompetitive inhibition is observed when SAM is the varied substrate, AcH4-21 is the fixed substrate (1 mM), and AcH4-21R3K is the dead-end analogue inhibitor. (D) Noncompetitive inhibition is observed when AcH4-21 is the varied substrate, SAM is the fixed substrate (15 μM), and sinefungin is the dead-end analogue inhibitor. (E) Competitive inhibition is observed when SAM is the varied substrate, AcH4-21 is the fixed substrate (1 mM), and sinefungin is the dead-end analogue inhibitor.

Scheme 1. Rapid Equilibrium Mechanism with Dead-End E–AcH4-21–SAH and E–SAM–MMA Complexes^a



^aIn the cPRMT5 catalyzed reaction, the substrates bind to the enzyme in a random fashion to generate a ternary complex. After methyl transfer, the reaction products are released in a random fashion to regenerate the free enzyme. Dead-end complexes, EAP = E–AcH4-21–SAH or EBQ = E–SAM–MMA, can be formed when either reaction product, SAH or the MMA-containing peptide, binds to the enzyme after the first substrate binds or after the first product has been released from the ternary complex.

lated species is less than 1 and takes place on the same time scale as SAM rebinding and the release of monomethylated peptide. Since transfer of the second methyl group is exceedingly slow (due to the high K_M for the monomethylated substrate), it will be critical to identify the factors that alter the processivity of the enzyme and promote substrate symmetric dimethylation, because this is the physiologically relevant PTM. Whether an interacting protein can improve the processivity of cPRMT5 is currently unknown, but the discovery of one would be an exciting avenue for future research, and these results provide the baseline for their discovery.

Finally, the results of our initial velocity, product, and dead-end inhibition studies indicate that cPRMT5 uses a rapid equilibrium random kinetic mechanism with dead-end EAP and EBQ complexes. The fact that PRMTs 1 and 6 also use the same type of mechanism^{26,32} suggests that this kinetic pathway may be a universal feature of the PRMTs. If that is the case, the use of a random mechanism of substrate binding and product release likely provides a mechanism to regulate enzyme activity by, for example, altering the product distribution patterns of the PRMTs, that is, the distribution of MMA, SDMA, and ADMA on a particular substrate. In total, these studies undoubtedly lay the foundation for studying the regulation of PRMT5 activity and will likely help guide the development of inhibitors targeting this medically relevant enzyme.

■ ASSOCIATED CONTENT

Supporting Information

Purification of cPRMT5 and cPRMT5 methylation of the AchH-21 peptide in a distributive fashion. This material is available free of charge via the Internet at <http://pubs.acs.org>.

■ AUTHOR INFORMATION

Corresponding Author

*Mailing address: Department of Chemistry, The Scripps Research Institute, Scripps Florida, 130 Scripps Way, Jupiter, FL 33458. Tel: (561)-228-2860. Fax: (561)-228-2918. E-mail: pthompso@scripps.edu.

Notes

The authors declare no competing financial interest.

■ ABBREVIATIONS

PTM, post-translational modification; PRMT, protein arginine methyltransferase; CARM1, coactivator-associated arginine methyltransferase 1; MMA, monomethylarginine; ADMA, asymmetric dimethylarginine; SDMA, symmetric dimethylarginine; NOS, nitric oxide synthase; MEP50, methylsome protein 50; CDK4, cyclin D1/cyclin-dependent kinase; EGFR, epidermal growth factor receptor; SHP1, SH2-domain-containing protein tyrosine phosphatase 1; PDCD4, programmed cell death protein 4; JAK2, Janus kinase 2; SAM, S-adenosyl-L-methionine; SAH, S-adenosyl-L-homocysteine; CORP5, cooperator of PRMT5; CEP-1, *C. elegans* p53-like protein 1

■ REFERENCES

- (1) Bedford, M. T., and Richard, S. (2005) Arginine methylation an emerging regulator of protein function. *Mol. Cell* 18, 263–272.
- (2) Hong, H., Kao, C., Jeng, M. H., Eble, J. N., Koch, M. O., Gardner, T. A., Zhang, S., Li, L., Pan, C. X., Hu, Z., MacLennan, G. T., and Cheng, L. (2004) Aberrant expression of CARM1, a transcriptional coactivator of androgen receptor, in the development of prostate carcinoma and androgen-independent status. *Cancer* 101, 83–89.

- (3) Leiper, J., Nandi, M., Torondel, B., Murray-Rust, J., Malaki, M., O'Hara, B., Rossiter, S., Anthony, S., Madhani, M., Selwood, D., Smith, C., Wojciak-Stothard, B., Rudiger, A., Stidwill, R., McDonald, N. Q., and Vallance, P. (2007) Disruption of methylarginine metabolism impairs vascular homeostasis. *Nat. Med.* 13, 198–203.
- (4) Majumder, S., Liu, Y., Ford, O. H., 3rd, Mohler, J. L., and Whang, Y. E. (2006) Involvement of arginine methyltransferase CARM1 in androgen receptor function and prostate cancer cell viability. *Prostate* 66, 1292–1301.
- (5) Vallance, P., and Leiper, J. (2004) Cardiovascular biology of the asymmetric dimethylarginine:dimethylarginine dimethylaminohydrolase pathway. *Arterioscler., Thromb., Vasc. Biol.* 24, 1023–1030.
- (6) Yang, Y., and Bedford, M. T. (2013) Protein arginine methyltransferases and cancer. *Nat. Rev. Cancer* 13, 37–50.
- (7) Bedford, M. T., and Clarke, S. G. (2009) Protein arginine methylation in mammals: Who, what, and why. *Mol. Cell* 33, 1–13.
- (8) Zurita-Lopez, C. I., Sandberg, T., Kelly, R., and Clarke, S. G. (2012) Human protein arginine methyltransferase 7 (PRMT7) is a type III enzyme forming omega-NG-monomethylated arginine residues. *J. Biol. Chem.* 287, 7859–7870.
- (9) Rust, H. L., and Thompson, P. R. (2011) Kinase consensus sequences: A breeding ground for crosstalk. *ACS Chem. Biol.* 6, 881–892.
- (10) Karkhanis, V., Hu, Y. J., Baiocchi, R. A., Imbalzano, A. N., and Sif, S. (2011) Versatility of PRMT5-induced methylation in growth control and development. *Trends Biochem. Sci.* 36, 633–641.
- (11) Kim, J. M., Sohn, H. Y., Yoon, S. Y., Oh, J. H., Yang, J. O., Kim, J. H., Song, K. S., Rho, S. M., Yoo, H. S., Kim, Y. S., Kim, J. G., and Kim, N. S. (2005) Identification of gastric cancer-related genes using a cDNA microarray containing novel expressed sequence tags expressed in gastric cancer cells. *Clin. Cancer Res.* 11, 473–482.
- (12) Goulet, I., Gauvin, G., Boisvenue, S., and Cote, J. (2007) Alternative splicing yields protein arginine methyltransferase 1 isoforms with distinct activity, substrate specificity, and subcellular localization. *J. Biol. Chem.* 282, 33009–33021.
- (13) Dacwag, C. S., Ohkawa, Y., Pal, S., Sif, S., and Imbalzano, A. N. (2007) The protein arginine methyltransferase Prmt5 is required for myogenesis because it facilitates ATP-dependent chromatin remodeling. *Mol. Cell. Biol.* 27, 384–394.
- (14) Cho, E. C., Zheng, S., Munro, S., Liu, G., Carr, S. M., Moehlenbrink, J., Lu, Y. C., Stimson, L., Khan, O., Konietzny, R., McGouran, J., Coutts, A. S., Kessler, B., Kerr, D. J., and Thangue, N. B. (2012) Arginine methylation controls growth regulation by E2F-1. *EMBO J.* 31, 1785–1797.
- (15) Jansson, M., Durant, S. T., Cho, E. C., Sheahan, S., Edelmann, M., Kessler, B., and La Thangue, N. B. (2008) Arginine methylation regulates the p53 response. *Nat. Cell Biol.* 10, 1431–1439.
- (16) Malkin, D., Li, F. P., Strong, L. C., Fraumeni, J. F., Nelson, C. E., Kim, D. H., Kassel, J., Gryka, M. A., Bischoff, F. Z., Tainsky, M. A., and Friend, S. H. (1990) Germ Line P53 Mutations in a Familial Syndrome of Breast-Cancer, Sarcomas, and Other Neoplasms. *Science* 250, 1233–1238.
- (17) Davison, T. S., Yin, P., Nie, E., Kay, C., and Arrowsmith, C. H. (1998) Characterization of the oligomerization defects of two p53 mutants found in families with Li-Fraumeni and Li-Fraumeni-like syndrome. *Oncogene* 17, 651–656.
- (18) Powers, M. A., Fay, M. M., Factor, R. E., Welm, A. L., and Ullman, K. S. (2011) Protein arginine methyltransferase 5 accelerates tumor growth by arginine methylation of the tumor suppressor programmed cell death 4. *Cancer Res.* 71, 5579–5587.
- (19) Aggarwal, P., Vaite, L. P., Kim, J. K., Mellert, H., Gurung, B., Nakagawa, H., Herlyn, M., Hua, X., Rustgi, A. K., McMahon, S. B., and Diehl, J. A. (2010) Nuclear cyclin D1/CDK4 kinase regulates CUL4 expression and triggers neoplastic growth via activation of the PRMT5 methyltransferase. *Cancer Cell* 18, 329–340.
- (20) Pal, S., Vishwanath, S. N., Erdjument-Bromage, H., Tempst, P., and Sif, S. (2004) Human SWI/SNF-associated PRMT5 methylates histone H3 arginine 8 and negatively regulates expression of ST7 and NM23 tumor suppressor genes. *Mol. Cell. Biol.* 24, 9630–9645.

- (21) Sun, L., Wang, M., Lv, Z., Yang, N., Liu, Y., Bao, S., Gong, W., and Xu, R. M. (2011) Structural insights into protein arginine symmetric dimethylation by PRMT5. *Proc. Natl. Acad. Sci. U. S. A.* 108, 20538–20543.
- (22) Yang, M., Sun, J., Sun, X., Shen, Q., Gao, Z., and Yang, C. (2009) *Caenorhabditis elegans* protein arginine methyltransferase PRMT-5 negatively regulates DNA damage-induced apoptosis. *PLoS Genet.* 5, No. e1000514.
- (23) Antonysamy, S., Bonday, Z., Campbell, R. M., Doyle, B., Druzina, Z., Gheyi, T., Han, B., Jungheim, L. N., Qian, Y., Rauch, C., Russell, M., Sauder, J. M., Wasserman, S. R., Weichert, K., Willard, F. S., Zhang, A., and Emtage, S. (2012) Crystal structure of the human PRMT5:MEP50 complex. *Proc. Natl. Acad. Sci. U. S. A.* 109, 17960–17965.
- (24) Ho, M.-C., Wilczek, C., Bonanno, J. B., Xing, L., Seznec, J., Matsui, T., Carter, L. G., Onikubo, T., Kumar, P. R., Chan, M. K., Brenowitz, M., Cheng, R. H., Reimer, U., Almo, S. C., and Shechter, D. (2013) Structure of the Arginine Methyltransferase PRMT5-MEP50 Reveals a Mechanism for Substrate Specificity. *PLoS ONE* 8, No. e57008.
- (25) Lacroix, M., El Messaoudi, S., Rodier, G., Le Cam, A., Sardet, C., and Fabbrizio, E. (2008) The histone-binding protein COPRS is required for nuclear functions of the protein arginine methyltransferase PRMT5. *EMBO Rep.* 9, 452–458.
- (26) Obianyo, O., and Thompson, P. R. (2012) Kinetic mechanism of protein arginine methyltransferase 6 (PRMT6). *J. Biol. Chem.* 287, 6062–6071.
- (27) Thompson, P. R., Kurooka, H., Nakatani, Y., and Cole, P. A. (2001) Transcriptional coactivator protein p300. Kinetic characterization of its histone acetyltransferase activity. *J. Biol. Chem.* 276, 33721–33729.
- (28) Osborne, T. C., Obianyo, O., Zhang, X., Cheng, X., and Thompson, P. R. (2007) Protein arginine methyltransferase 1: positively charged residues in substrate peptides distal to the site of methylation are important for substrate binding and catalysis. *Biochemistry* 46, 13370–13381.
- (29) Pal, S., Baiocchi, R. A., Byrd, J. C., Grever, M. R., Jacob, S. T., and Sif, S. (2007) Low levels of miR-92b/96 induce PRMT5 translation and H3R8/H4R3 methylation in mantle cell lymphoma. *EMBO J.* 26, 3558–3569.
- (30) Branscombe, T. L., Frankel, A., Lee, J. H., Cook, J. R., Yang, Z., Pestka, S., and Clarke, S. (2001) PRMT5 (Janus kinase-binding protein 1) catalyzes the formation of symmetric dimethylarginine residues in proteins. *J. Biol. Chem.* 276, 32971–32976.
- (31) Gui, S., Wooderchak-Donahue, W. L., Zang, T., Chen, D., Daly, M. P., Zhou, Z. S., and Hevel, J. M. (2013) Substrate-induced control of product formation by protein arginine methyltransferase 1. *Biochemistry* 52, 199–209.
- (32) Obianyo, O., Osborne, T. C., and Thompson, P. R. (2008) Kinetic mechanism of protein arginine methyltransferase 1. *Biochemistry* 47, 10420–10427.